

PHYSICAL REVIEW D

PARTICLES AND FIELDS

THIRD SERIES, VOLUME 24, NUMBER 7

1 OCTOBER 1981

Study of highly ionizing particles at mountain altitude

K. Kinoshita and P. B. Price

Department of Physics and Space Sciences Laboratory, University of California, Berkeley, California 94720

(Received 27 April 1981)

The inspiration for this experiment was the widely acknowledged peculiar nature of the "Centauro" class of ultrahigh-energy interactions discovered at Mt. Chacaltaya about a decade ago by a Brazil-Japan collaboration. The rate of Centauro events is quite low, $\sim 0.02 \text{ m}^{-2}\text{yr}^{-1}$. Among the proposed explanations is the possibility that they might be initiated by a highly charged primary particle. To look for such particles we deployed a series of CR-39 plastic track detectors with large collecting power at the summit of White Mountain, California (603 g/cm^2). Two experiments have been completed and analyzed: a single layer with a $10\text{-m}^2\text{yr}$ exposure, and three layers in coincidence with a $0.025\text{-m}^2\text{yr}$ exposure. In the first experiment, the single layer was adopted to maximize the collecting area at some sacrifice in velocity information. The results demonstrate the superiority of CR-39 as a detector of highly ionizing particles ($Z/\beta \gtrsim 30$) and its particular suitability as a collector of very rare particles. The performance of the plastic was evaluated by examining the high density of tracks due to slow, light ions. The low-energy spectra of nuclei with $Z \leq 3$ have been measured and are found to be consistent with spectra calculated from a model where the source of ions is atmospheric collisions of energetic hadrons. This is the first time that energetic Li has been identified at mountain altitude and that enough He has been seen to permit measurements of its energy spectrum. A density $\sim 10 \text{ m}^{-2}$ of fast particles with $Z \geq 4$ found in individual layers is consistent with the exposure received in a 10-hour commercial jet flight. A fast-scanning method was used to examine the entire single-layer array. In the interval $30 \lesssim Z/\beta \lesssim 100$, no events were found, from which we infer an upper limit of $0.4 \text{ m}^{-2}\text{yr}^{-1}$ (95% C.L.) on the flux of electrically charged particles with $Z/\beta \sim 30$ to ~ 100 and on the flux of superheavy magnetic monopoles with $\beta \gtrsim 0.02$. Two objects were located which, if they are indeed tracks, would correspond to particles with $Z/\beta \gtrsim 100$, with abundance $\sim 0.2 \text{ m}^{-2}\text{yr}^{-1}$. Without sheets in coincidence, it is impossible to distinguish these objects from certain flaws in the plastic. A new detector, with three layers interleaved with absorbers and with an area of 20 m^2 , will correct this shortcoming and be able to measure the spectra of light elements to higher energies as well.

I. INTRODUCTION

The Earth's atmosphere serves as an effective filter of energetic complex nuclei in the cosmic rays. The nuclear-interaction mean free path in air is $\sim 75 \text{ g/cm}^2$ for protons, decreasing to $\sim 13 \text{ g/cm}^2$ for iron, and is even shorter for heavier elements. The depth of the atmosphere ranges from $\sim 10^3 \text{ g/cm}^2$ at sea level to 540 g/cm^2 at the highest ground-based cosmic-ray observatory, on Mt. Chacaltaya. As a result of the preferential exponential absorption of heavier primaries with depth in the atmosphere, the surviving primary cosmic rays at mountain altitude consist almost exclusively of protons. The majority of the high-energy secondary hadrons are neutrons, protons, and pions. Consequently, one has, at mountain altitude, a ground-based observatory with virtually complete filtering of primary cosmic-ray nuclei

with $Z \gtrsim 2$, while retaining a much greater flux of particles with longer interaction lengths than would be available at sea level. Thus, at mountain-top observatories one can use detectors of large area to study elementary-particle interactions at energies up to almost 10^{16} eV , well beyond the reach of accelerators. The mountain top is also an attractive location to search for a low flux of any particles with unusual characteristics such as high mass¹ or fractional charge.²

A Brazil-Japan collaboration has employed a 44-m^2 , two-story emulsion chamber at Mt. Chacaltaya for the study of ultraenergetic interactions. With this chamber, the group has seen, over the last decade, several unusual events named by them "Centauro."³ These events, of energy $\gtrsim 1000 \text{ TeV}$, are characterized by high transverse momentum and high hadron multiplicity ($\sim 10^2$) but with essentially no π^0 's, i.e., no γ showers observed.

Some of the attributes of this type of event could be accounted for by the breakup of a heavy ($\sim 10^2$ amu) primary nucleus, but recent calculations have shown⁴ that only nuclei with $Z \lesssim 7$ have a flux comparable to or larger than the flux of Centauros, $\sim 0.02 \text{ m}^{-2}\text{yr}^{-1}$, at the altitude of Mt. Chacaltaya. Simulations have demonstrated that neutral-pion production as infrequent as seen in the Centauros is not a statistical fluctuation of proton-induced interactions.⁵ One possible explanation is that new interaction mechanisms become important at very high energies. Other models which might explain Centauros call for exotic primary particles—quark droplets,⁶ superdense nuclei,⁷ hyperstrange quark states,⁸ or hypothetical elementary particles.⁹ The charge of the primary is not known from data at Chacaltaya, and predictions based on the proposed models vary from essentially zero to $\sim 10^2 e$. Because the interaction length of the particle is not known, its flux at mountain altitude is quite uncertain. The observations at Chacaltaya indicate that ~ 0.02 particles $\text{m}^{-2}\text{yr}^{-1}$ interact in ~ 1 km, or 50 g/cm^2 , of atmosphere above the detector. Assuming exponential absorption, the ratio of the flux of Centauro interactions, ϕ_{Cent} , to the flux of surviving particles at Chacaltaya, ϕ_{Surv} , is

$$\phi_{\text{Cent}}/\phi_{\text{Surv}} = e^{\delta/\lambda} - 1, \quad (1)$$

where λ is the interaction length in g/cm^2 and δ is the event-sampling thickness, $\sim 50 \text{ g/cm}^2$. If λ is greater than $\sim 50 \text{ g/cm}^2$, the flux of particles surviving to mountain altitude is expected to be of at least the same order of magnitude as the flux of events observed at Chacaltaya. The surviving particles in the chamber at Chacaltaya, however, would not be observed, even if they were highly charged; due to the practical impossibility of microscopically scanning 44 m^4 , the emulsion is not examined unless there is a macroscopic shower spot in the x-ray film just above it.

Of the experiments that might have a bearing on the question of the origin of the Centauro events, no search at mountain altitude has had both a large collecting power and the ability to resolve single, highly charged particles. One sea-level magnetic-monopole search¹⁰ has collected an integrated flux of $18 \text{ m}^2\text{yr}$. The Lexan plastic track detector in that experiment was insensitive to $Z \lesssim 65$. Thus, a large range of intermediate charges, $7 \lesssim Z \lesssim 65$, for which the expected flux of surviving cosmic rays is significantly lower than the Centauro flux, has not been explored.

The recent development of the CR-39 plastic track detector,¹¹ which is capable of recording tracks of particles with $Z/\beta \gtrsim 10$ ($\beta \equiv v/c$), makes it possible to search for rare particles over most

of this unexplored charge region below $Z = 65$. We report here the results of the first of a series of experiments being conducted with layers of CR-39, $\sim 600 \mu\text{m}$ thick, exposed at White Mountain Research Station (603 g/cm^2) and at Mt. Chacaltaya. Using a rapid-scanning technique to cover many square meters, we have begun to explore the charge region $Z/\beta \gtrsim 30$ and, with a high-magnification microscope scan, have seen a high density of low-energy secondary particles with $Z \lesssim 3$ and have begun to measure their energy spectra. We have collected data for hydrogen, helium, and lithium from our first exposure of $10 \text{ m}^2\text{yr}$ and are able to compare our spectra with the spectrum of hydrogen and the few counts of helium recently obtained¹² at Mt. Lemmon in Arizona (750 g/cm^2).

II. SENSITIVITY OF PLASTIC TRACK DETECTORS AND METHODS OF LOCATING EVENTS

Plastic track detectors have very significant advantages over either nuclear emulsions or electronic detectors for the study of highly ionizing particles at very low event rates in a background of lightly ionizing particles.¹³ Figure 1 compares the sensitivities of Lexan polycarbonate, which had been used in a previous search for sea-level magnetic monopoles,¹⁰ and of three varieties of CR-39 allyl diglycol carbonate. Here we define sensitivity, $s \equiv \text{csc}\theta_c = v_T/v_G$, as the ratio of the chemical etching rate v_T along the radiation-damaged material defining the particle trajectory, to the general etching rate v_G of the plastic itself. The semicone angle θ_c of the resulting etch pit is equal to $\arcsin(v_G/v_T)$. Using heavy-ion beams at the Lawrence Berkeley Laboratory 88-in. cyclo-

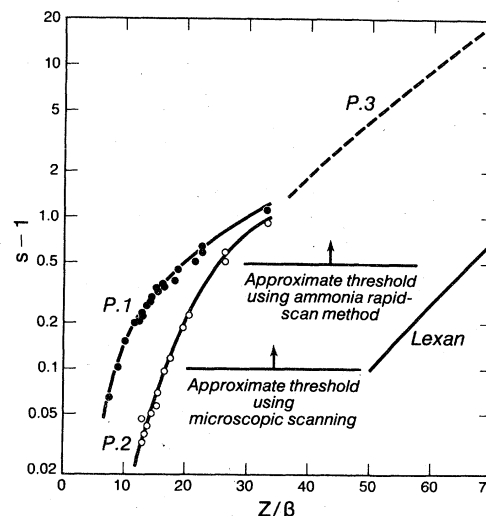


FIG. 1. Response of Lexan and of three batches of CR-39 as a function of Z/β . The quantity s is the ratio of track etch rate to general etch rate.

tron, we determined the dependence of s on Z/β in Fig. 1 for two varieties of CR-39 made to our specifications by Pershore Mouldings, Ltd. (labeled P.1 and P.2). We used batch P.1 in a large-area, single-layer experiment and batch P.2, which contained 1% of an organic additive that gave it a more uniform post-etch surface,¹⁴ for a small, multilayer experiment. The dashed curve labeled P.3 refers to data at higher ionization rates obtained on CR-39 made by Pershore several years ago.

The two horizontal lines in Fig. 1 show the approximate minimum values of s that can be detected by two different scanning techniques. Scanning microscopically with a 20 \times objective, at a total magnification of $\sim 300\times$, one can see etch pits at s as low as 1.1 (or $s - 1 = 0.1$) on either the top or bottom surface of a sheet of thickness up to ~ 1.5 mm and can thus locate trajectories of particles that pass through a detector and produce etchable pits on both surfaces. The dimensions of the top and bottom members of a correlated pair can be measured as each event is located. This scanning method is well suited for a study of relatively frequent events down to a limiting s of 1.1, corresponding to $Z/\beta \geq 9$ or 10 for batch P.1 or to $Z/\beta \geq 16$ or 17 for batch P.2, but the rate of area scanning is slow, about 1 cm² per hour. For a 1-yr exposure and 100 h of scanning, the lowest flux one can detect with this method is $\sim 10^2$ particles per m²yr.

The second method is much faster but is capable of detecting only events with considerably higher Z/β . It is desirable to employ at least two layers of CR-39, one for scanning and one for accurate measurement. The detector to be scanned is etched for a very long time such that its thickness is reduced from H_i to a final thickness H_f . The criterion for the two etch pits to meet in the middle and form a hole is that $\frac{1}{2}(s_{\text{top}} + s_{\text{bottom}}) \cos \theta_z \geq H_i(H_i - H_f)^{-1}$, where θ_z is the zenith angle of the event. Because of thickness variations in a detector, it is impractical to etch it until its final thickness is less than about one-third its initial average thickness, which leads to the practical limitation that only events with average s greater than ~ 1.5 will be located by this method. The distribution of etched holes in a sheet is determined by sealing ammonia-sensitive paper between the sheet and a smooth surface, with the sensitive side of the paper facing the sheet, passing ammonia gas over the sheet, and noting the positions of blue spots on the ammonia paper.¹³ A second layer is etched for the normal time, so that the etch pits do not meet, and the pits corresponding to holes in the heavily etched layer are then measured microscopically.

In the present experiment we have also used a third scanning method of intermediate sensitivity. This involves scanning a sheet in a stereomicroscope at a magnification of 50 \times to 150 \times . Correlated pairs with $s \geq 1.25$ can be detected at a rate of about 10 to 20 cm² per hour.

Repeated scans showed that scanning microscopically at 300 \times gives an efficiency indistinguishable from unity for $s \geq 1.1$ and that the ammonia technique reveals the same events repeatedly. Scanning in a stereomicroscope reveals etch-pit pairs with $s \geq 1.25$ with an efficiency that varies from ~ 0.9 to essentially unity depending on local surface roughness and transparency.

III. EXPOSURES AND EXPERIMENTAL RESULTS

A. Search for particles with $Z/\beta \geq 30$

Because of budgetary limitations, and in order to maximize collecting power for rare events that might account for the Centauro phenomenon, we decided to do initial searches with single layers of large area both at Mt. Chacaltaya in Bolivia and at White Mountain in California. The reason for preferring a single layer of area A to n layers of area A/n is that if only one or two interesting events were to be found in area A , even though they could not be accurately identified (one layer having to be overetched in order to locate events by the ammonia method), there would be great motivation to conduct a more expensive follow-up experiment with greater area, multiple layers, and interleaved absorbers. With n layers of area A/n we might find no events and never continue the search.

All CR-39 detectors were shipped from London to San Francisco in a 10-h flight. The overlying material was 250 g/cm² of air plus an unknown (probably less than 5 g/cm²) thickness of solid matter.

We arranged to have a single 12-m² layer of CR-39 from batch P.1 mounted on top of a freshly prepared emulsion chamber at Mt. Chacaltaya, beginning on 18 April 1980. To exclude fresh air containing radon that would produce a background of α -particle tracks, and to protect the detector surfaces from scratches, each 0.15-m² sheet of CR-39 was vacuum heat-sealed in a polyethylene bag. In collaboration with members of the Brazil-Japan emulsion groups, we plan to follow interesting events found either in CR-39 or in the emulsion chamber into the other detector. Political difficulties in Bolivia have prevented us from retrieving the CR-39, and the exposure will continue longer than we had planned. The CR-39 can store tracks for many years at room temperature without any deterioration.

We exposed a 15-m² layer of CR-39 from batch P.1, heat-sealed in polyethylene, inside a cabin at the summit of White Mountain beginning in October 1979. After a 6-month exposure we recovered 6 m² and etched it for 4 days at 70 °C in a 6.25 normal sodium hydroxide solution. After a 9-month exposure we recovered the remaining 9 m² and etched it for 4 days at 70 °C. Under these conditions the sheet thickness decreased by about 290 μm. Essentially all of the sheets had initial thicknesses from 500 to 700 μm. The few thinner than about 500 μm tended to break during etching and fall into the stirring propeller. Individual sheets vary in thickness by about 10%.

The ammonia technique was used to scan an area of ~12 m² of the surviving sheets. We found a total of ~200 irregular tubular holes that probably resulted from rapid etching of dust fibers that did not get filtered out of the liquid monomer from which batch P.1 was polymerized. These holes are instantly recognizable in a low-power stereomicroscope as artifacts unrelated to tracks.

We also found two perfectly straight cylindrical holes, with no perceptible taper, that are consistent with the sizes and shapes of etched, connecting pits due to extremely highly ionizing particles. Their diameters are $2v_c t = 0.29$ mm, where t = etch time, and their intercepts with the surfaces have the ellipticity expected for their zenith angles. In the case of a genuine track, two etch pits that connect from opposite surfaces taper in diameter to a minimum at the center, the angle of taper being given by $\csc\theta_c = s$. We estimate that if charged particles were responsible for these etched holes, they must have had $Z/\beta \approx 100$. Such highly charged objects might, by disintegrating above a detector, give rise to the Centauro phenomenon.

Rather than express regret that we did not have a second layer that could have been used to test whether the two cylindrical holes were due to tracks or flaws, we argue that if two layers 7.5 m² in area had been superimposed, and if the

events are real, they might have missed the 7.5-m² array and we would have had no motivation for planning a second, larger, multilayer array.

Using the relation $\frac{1}{2}(s_{\text{top}} + s_{\text{bottom}}) \cos\theta_x \geq H_i(H_i - H_f)^{-1}$, together with $H_i = 500$ to 700 μm and $H_i - H_f = 290$ μm, and the dependence of s on Z/β for batch P.1 in Fig. 1, we conclude that the flux of particles with Z/β between ~30 and ~10² is less than ~0.4 per m² per yr (at 95% C.L.) and that we cannot rule out a small but finite flux of particles with $Z/\beta \approx 10^2$.

B. Measurements of H and He nuclei with $10 \leq Z/\beta \leq 30$

The plastic detectors exposed at White Mountain for 6 and 9 months recorded a high density of single etch pits, ~200/cm² and ~300/cm², respectively, on each surface. The density of these pits is quite consistent with the rate of production of short-range (≤ 500 μm) fragments by energetic secondary hadrons colliding with N and O nuclei in the air above the detectors and with C and O nuclei in the plastic detectors. "Target fragmentation" is the term used to refer to this process, which is usually modeled by assigning a temperature and mean recoil velocity to the target nucleus.

The White Mountain detectors also recorded a large number, ~10/cm², of pairs of etch pits on top and bottom surfaces, aligned with one another to within measurement errors of ~1° and peaked at very small zenith angles. The expected density of etch-pit pairs due to projectile fragmentation of primary heavy cosmic rays (Fig. 7 and Table I) is far lower than this. We will show later that the vast majority of these etch-pit pairs, due to particles that pass through the sheets, are produced by fragmentation of air nuclei by secondary hadrons, dominantly neutrons and protons. Those due to particles that have barely enough energy to pass through the detector form the high-energy tail of the target evaporation spectrum that is responsible for the single pits, whereas those due to particles

TABLE I. Expected density of etch-pit pairs in CR-39 due to multicharged fragments of cosmic-ray nuclei ($0^\circ \leq \theta_z \leq 25^\circ$).

Nucleus	$\lambda_{\text{int}}(\Delta A \geq 1)$ (g cm ⁻²)	Expected density (m ⁻²)		
		9 months at 603 g cm ⁻² $Z/\beta \geq 10$	10 h at 250 g cm ⁻² $Z/\beta \geq 10$	$Z/\beta \geq 15$
He	42	< 24 ^a	42	4
Li	36	0.5	23	4
Be	34	0.2	26	5
B	29	0.06	23	4
C	27	0.015	13	2
N	26	1.5×10^{-3}	7	1.4
Ne	22	1.2×10^{-5}	0.36	0.16

^aGeomagnetic field would exclude some of the parents.

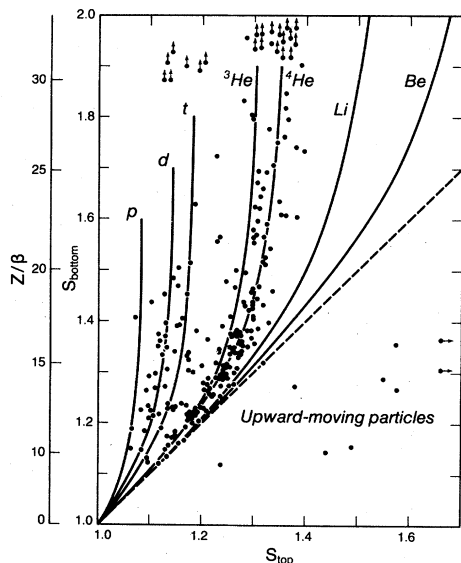


FIG. 2. Measurements of top and bottom values of s for etch-pit pairs found in an 18-cm² area. The Z/β scale along the ordinate applies both to s_{bottom} and s_{top} .

of higher energy are produced by direct, non-thermal reactions.

Figure 2 shows data from a microscopic scan of 18 cm² of a sheet exposed at White Mountain for 9 months. Each data point gives two parameters, s_{top} and s_{bottom} , from which both Z and β can be separately calculated if the range difference $H_i \sec \theta_x$ is known. The values of s_{top} , s_{bottom} , H_i , and θ_x are determined from microscopic measurements of the top and bottom etch pits. Because H_i was reasonably constant over the small area from which the measurements in Fig. 2 were taken, and because $\sec \theta_x$ is approximately unity for all events, hydrogen and helium events are reasonably well resolved on this simple two-parameter plot of s_{top} and s_{bottom} , even before correcting for variations in $H_i \sec \theta_x$. The curves labeled p , d , t , ${}^3\text{He}$, and ${}^4\text{He}$ were calculated from the dependence of s on Z/β in Fig. 1, assuming the average value $H_i \sec \theta_x = 550 \mu\text{m}$.

We note several features in Fig. 2. Although the great majority of the particles were directed downward ($s_{\text{bottom}} > s_{\text{top}}$), there is a small flux of low-energy, upward-moving ($s_{\text{top}} > s_{\text{bottom}}$) fragments of interactions of cosmic rays in the polyethylene below the detector. This is to be expected, because the angular distribution in target fragmentation extends, for low-energy fragments, into the backward hemisphere.¹⁵⁻¹⁷ Although the flux of protons greatly exceeds the fluxes of other charged particles, almost no etch-pit pairs due to protons were recorded. Only that small fraction of protons that have very small θ_x and barely penetrate the bottom of the detector have a high enough ionization rate

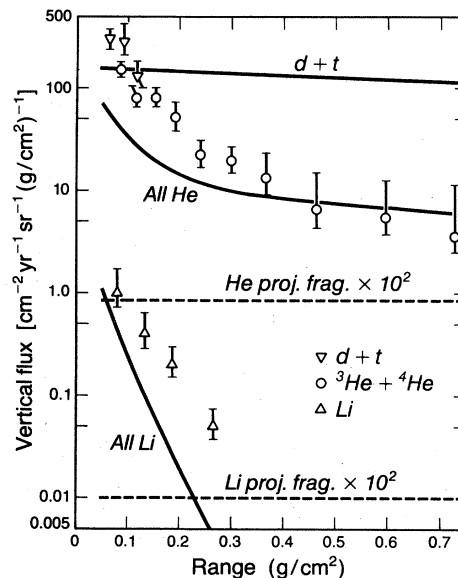


FIG. 3. Differential range spectra of nuclei observed at White Mountain. Error bars (68% C. L.) are due to counting statistics. Calculated range spectra for production by collisions of secondary hadrons with air (solid curves) and for projectile fragments of primary heavy cosmic rays (dashed curves, from Fig. 7) are shown.

at the top of the detector to produce an etchable track. No particles with $Z > 2$ were conclusively identified in the 18-cm² scan. One candidate, with $s_{\text{top}} = s_{\text{bottom}} = 1.32$ and $Z/\beta = 15$, appeared to have a high β and $Z \approx 4$, but with only one pair of measurements of s we cannot rule out the possibility that it was caused by a helium nucleus with an abnormally large deviation of response of the CR-39 from the calculated ${}^4\text{He}$ curve.

From the measurements of events found in the 18-cm² scan we have calculated the differential range spectra of $d+t$ and of He nuclei in particles per cm² per year per steradian per g/cm² of air, using data at zenith angles $0^\circ \leq \theta_x \leq 25^\circ$ and at values of $Z/\beta \geq 9$. The results are plotted in Fig. 3. The range spectra have been converted to differential energy spectra, shown in Fig. 4, so that the data can be compared with spectra at higher energies reported by Barber *et al.*¹² and with spectra calculated to result from various reactions of secondary hadrons with air nuclei. The curves in Figs. 3 and 4 will be discussed in Sec. IV.

C. Measurements of nuclei with $Z \geq 3$ and with $10 \leq Z \leq 30$

We used a low-power stereomicroscope to scan an area of 650 cm² for events with $Z \geq 3$. To eliminate deuterons, tritons, and most of the He nuclei, we accepted only etch-pit pairs for which the diameter of the top cone exceeded a size such that $s_{\text{top}} > 1.25$. This scan yielded a total of 10 possible

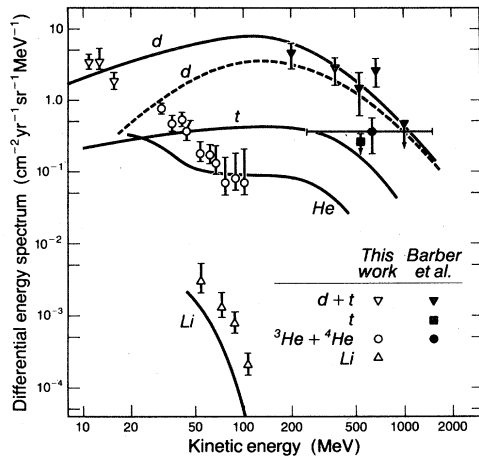


FIG. 4. Differential energy spectra of nuclei observed at White Mountain (603 g cm^{-2}). Solid curves are our calculated spectra; dotted curve and solid data points are from Barber *et al.* (Ref. 9), scaled up by a factor 3.2 to convert from their location at 747 g cm^{-2} to our location at 603 g cm^{-2} .

Li nuclei with $Z/\beta \geq 14$ and one event with $s_{\text{top}} \approx s_{\text{bottom}} \approx 1.6$, corresponding to $Z/\beta \approx 25$. Figure 5 shows the results. The curves labeled He, Li, and Be are identical to those in Fig. 2. The one event with $Z/\beta \approx 25$ appears to be significantly faster and more highly charged than the others. At $s \approx 1.6$ the standard deviation for a single etch pit is $\sigma_s \approx 0.04$, which constrains its charge to be $Z \approx 5$ but does not permit its direction of motion to be unambiguously determined.

To resolve events with $3 \leq Z \leq 5$, which appeared

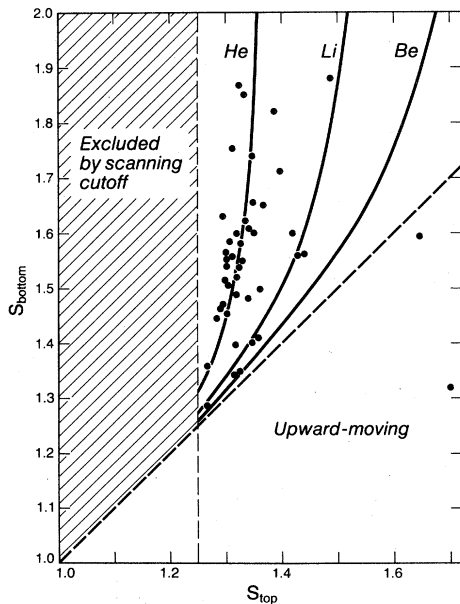


FIG. 5. Results of a biased scan for events with $Z \geq 3$, using the criterion $s_{\text{top}} > 1.25$. See text.

from the first exposure to occur at a rate of $\sim 100/\text{m}^2\text{yr}$, we exposed a small, multilayered stack. Batch P.2 was used, because, with its lower sensitivity and steeper response curve, it was expected to discriminate efficiently against H and He nuclides. The stack, three layers thick and 0.1 m^2 in area, was exposed for 3 months at the summit of White Mountain beginning in July 1980. Figure 6 shows the data for etch-pit pairs found in a stereomicroscopic scan of the entire stack. Deuterons and tritons are incapable of recording on both surfaces, and only those helium nuclei near the very end of their range are detected. The higher threshold and greater transparency of batch P.2 greatly speed up scanning. Lithium nuclei with $Z/\beta \geq 16$ are detected with efficiency comparable to that for stereomicroscopically locating Li with $Z/\beta \geq 14$ in the detectors made from batch P.1. The ratio of He to Li events for P.2 (Fig. 6) is lower than that for P.1 (Fig. 5) because of the higher detection threshold of P.2. Several of the events penetrated two sheets and one Li event penetrated all three sheets, proving that they occurred at 603 g/cm^2 rather than in the earlier 10-h flight at 250 g/cm^2 .

The events in both Figs. 5 and 6 were used to compute the differential range spectrum of Li in Fig. 3 and the differential energy spectrum in Fig. 4.

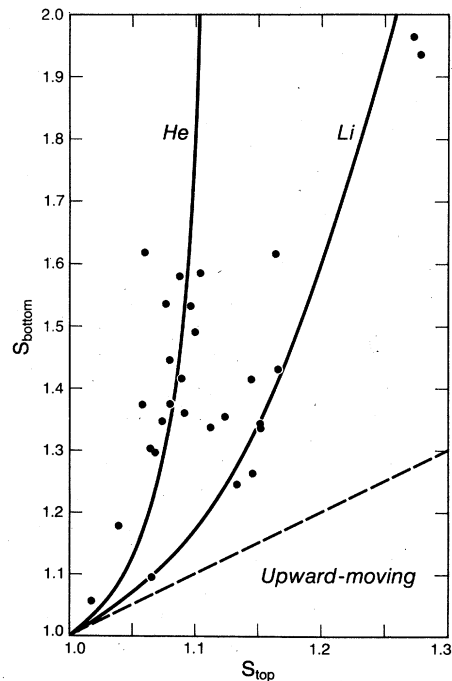


FIG. 6. Measurements of etch-pit pairs in stack P. 2. See text.

IV. CALCULATED FLUXES OF HIGHLY IONIZING PARTICLES IN THE ATMOSPHERE

A. Projectile fragmentation of primary cosmic-ray nuclei

Recently, Price *et al.*⁴ calculated the expected integral fluxes of fragments of cosmic-ray nuclei with charge $5 \leq Z \leq 28$ at various depths in the Earth's atmosphere, taking into account the initial energy and charge distributions, ionization loss, and various modes of fragmentation, and considering only the "projectile fragments," which have, to an excellent approximation, the same velocity as the primary particle. We have extended their calculations to $Z=2, 3$, and 4. In contrast to the nuclei with $Z \geq 3$, which are produced via a whole network of possible fragmentation chains, He is so abundant in the primary cosmic rays and has such a long interaction length ($\lambda_{\text{int}} = 42 \text{ g cm}^{-2}$) that the fragmentation network is quite simple. The dominant sources are surviving primary ${}^4\text{He}$ and secondary ${}^3\text{He}$ and ${}^4\text{He}$ from reactions ${}^4\text{He} + \text{air} \rightarrow {}^3,4\text{He} + X$. To estimate the contribution of secondary He we calculated the total cross sections for ${}^4\text{He} + \text{C} \rightarrow {}^3\text{He} + X$ and ${}^4\text{He} + \text{C} \rightarrow {}^4\text{He} + X$ from the differential cross sections measured by Anderson¹⁸ and defined an attenuation length $\Lambda \equiv \lambda_{\text{int}}(1-f)^{-1}$, where $f \approx 0.26$ is the fraction of interactions leading to ${}^3\text{He}$ or ${}^4\text{He}$.

Figure 7 shows the expected differential fluxes

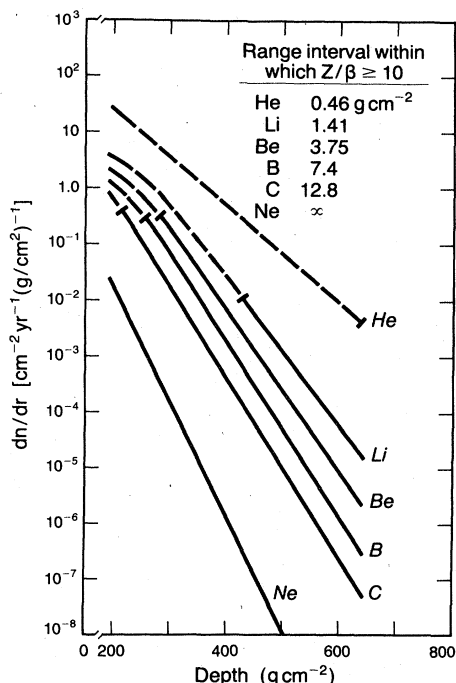


FIG. 7. Calculated differential range spectrum of projectile fragments of primary heavy cosmic rays as a function of depth in the Earth's atmosphere. See text.

of He, Li, Be, B, and C nuclei coming to rest at various depths in units of particles $\text{cm}^{-2}\text{yr}^{-1}(\text{g}/\text{cm}^2)^{-1}$, ignoring geomagnetic cutoff effects. These fluxes are strictly valid only at high geomagnetic latitudes. At White Mountain Research Station, where vertically incident cosmic rays with magnetic rigidity less than 4.5 GV/c are filtered out, some low-energy light nuclei that would otherwise contribute fragments are missing from the cosmic-ray beam. The dashed portions of the curves in Fig. 7 indicate where the fluxes of nuclei at the latitude of White Mountain are overestimated because of failure to take into account the geomagnetic cutoff.¹⁹ At the summit of White Mountain (603 g/cm^2), only the He nuclei are overestimated in Fig. 7. However, at the research station at Mt. Chacaltaya (540 g/cm^2), nuclei with rigidities up to 13.1 GV/c are filtered out and all of the fluxes in Fig. 7 are severe overestimates.

The point of this graph is to show that at mountain altitudes the fluxes of nuclei resulting from projectile fragmentation of primary cosmic-ray nuclei even as abundant as He are extremely low unless there exists some unknown collision mechanism that bestows upon some fraction of the products an anomalously long mean free path for subsequent interactions. Friedlander *et al.*²⁰ have recently discovered that some fraction of the products of projectile fragmentation have an anomalously short mean free path for subsequent interactions, an effect that would attenuate multicharged fragments even more strongly than Fig. 7 indicates.

For the CR-39 plastic detectors used in the present experiment, particles incident at zenith angles θ_z less than $\sim 25^\circ$ are detected with 100% efficiency if the ratio of charge to velocity satisfies the inequality $Z/\beta \geq 10$. Thus, nuclei with $Z < 10$ can be detected only within a limited interval of range ΔR . Values of ΔR for several nuclei are tabulated in Fig. 7. To estimate the number of projectile fragments of type Z that would be recorded per cm^2 per year, the appropriate curve in Fig. 7 can be integrated from the depth d at which the detector is situated to a depth $d + \Delta R$.

Table I gives the expected number of projectile fragments recorded per m^2 in a 9-month exposure at White Mountain (column 3), as well as in a 10-h exposure at a depth of 250 g/cm^2 , for $Z/\beta \geq 10$ (column 4) and for $Z/\beta \geq 15$ (column 5). We conclude that the densities of events recorded in CR-39 due to nuclei with $Z \geq 3$ are expected to be less than $1 \text{ m}^{-2}\text{yr}^{-1}$ at the summit of White Mountain if attenuated by known processes. Thus, the Earth's atmosphere effectively filters out primary cosmic rays and their projectile fragments with $Z \geq 3$. The last two columns show, however, that much greater densities of events with $Z \geq 3$ can accumu-

late in a single 10-h commercial air flight at a depth of 250 g/cm². All of the detectors used in the present experiment contain such a background as a result of having been flown from London to San Francisco. Most of the measured event densities reported above are much higher than predicted in Fig. 7 and Table I, and we attribute them to fragmentation of air nuclei by secondary hadrons. In contrast to the multicharged nuclei, the secondary hadrons have such long interaction lengths that the event densities originating in their collisions with air nuclei in 9 months at 603 g/cm² far outweigh the event densities accumulated in 10 h at 250 g/cm². It is easy to reject background from a jet plane flight if one demands that events pass through a stack assembled at the summit of White Mountain.

B. Interactions of secondary hadrons with air

In Fig. 3 it is easy to see that projectile fragmentation of primary heavy cosmic rays (dashed lines) fails by several orders of magnitude to account for the He and Li we have detected. We have calculated the spectra of *d*, *t*, He, and Li ejected from air nuclei by secondary hadrons and find that the results, shown as solid curves in Figs. 3 and 4, appear to be consistent with our data within the approximations we have had to make.

In our model various hadrons with known energy spectra collide with stationary targets at various heights above the detector, producing fragments with known energy (and range) distribution. The residual range at the detector is, of course, the initial range minus the height of the target above the detector. To generate the differential range spectra represented by the solid curves in Fig. 3, we integrated the contributions at each value of range from the continuous distribution of air at various heights above the detector. In addition to ionization loss, we have taken into account fragmentation of the fragments, which becomes increasingly important at energies above ~200 MeV.

The dominant target nuclei are N and O; the fragments of interest are *d*, *t*, ³He, ⁴He, and Li; most of the fragments we detect are made by neutrons and protons with energy between ~400 MeV and a few GeV; pions and other mesons make a negligible contribution. The differential cross sections for producing fragments at energies up to ~100 MeV are approximately independent of the projectile energy in this interval.^{15, 21, 22} At energies above ~10 GeV the hadron fluxes become negligible; below ~400 MeV both the total cross section and the maximum energy of the fragments drop rapidly.²²

We assume that the cross section for fragment

production in the energy interval of interest, ~10 to ~400 MeV, is zero for hadron kinetic energy below 400 MeV and energy-independent at all higher energies. The vertical intensities of neutrons and protons above 400 MeV at 603 g/cm² and a cutoff rigidity of 4.5 GV/c are ~1.3 × 10⁻² cm⁻²sr⁻¹s⁻¹ and 2 × 10⁻³ cm⁻²sr⁻¹s⁻¹, respectively.²³ We adopt a hadron flux of 0.015 cm⁻²sr⁻¹s⁻¹ (*E* > 400 MeV), which is consistent to within ~25% with values reported in other references.^{24, 25} The angular distribution at depth *x* falls off approximately as (cos θ_{*x*})^Λ, where Λ ≈ 125 g/cm² for protons and 155 g/cm² for neutrons.²³ At *x* = 603 g/cm², despite the fact that there is a substantial contribution at greater angles, we include only hadrons within 0° ≤ θ_{*x*} ≤ 30°, which leads to a total hadron flux of 9 × 10⁻³ cm⁻²s⁻¹ (*E* > 400 MeV) when integrated over solid angle. The reason for neglecting larger angles is that our observed fluxes of *d*, *t*, He, and Li fall off very rapidly at θ_{*x*} > 30°, and the angular distribution of energetic fragments such as these in hadron collisions with nuclei is strongly forward-peaked. Fragments produced by hadrons of large θ_{*x*} will tend to have the same large θ_{*x*} themselves and will thus have to pass through more matter to reach our detector.

A large body of cross-section data exists for protons on carbon and aluminum targets. We assumed identical cross sections for proton and neutron projectiles. To find cross sections for air we interpolated between C and Al targets. For fragment energies up to ~75 MeV we used the Maxwellian-type expressions, temperatures, and total cross sections found by Westfall *et al.*,¹⁵ supplemented by the data of Alard *et al.*²¹ and Bogatin *et al.*²² The proton beam energies were 2.1 and 4.9 GeV for Ref. 15, 600 MeV for Ref. 21, and 660 MeV for Ref. 22. Our Li data extend beyond energies for which data obtained at proton accelerators exist. If we were simply to extend the Maxwellian expression of Westfall *et al.* to higher energies, keeping the same temperature, τ = 13 MeV, we would underestimate our Li flux by a large factor. Both in their work and in earlier work by Korteling *et al.*¹⁶ and by Poskanzer *et al.*,¹⁷ it is clear that light isotopes of He, Li, and Be cannot be fit by the single Maxwellian. The cross section deviates more and more above a Maxwellian with increasing temperature. Guided by these references and by the results of Gaidos *et al.*,²⁶ we used a temperature of 13 MeV to fit Li data up to 30 MeV, joined smoothly to a Maxwellian at a temperature of 20 MeV, to predict approximate production rates from 30 to 110 MeV, the interval over which we have data.

For *d*, *t*, ³He, and ⁴He fragments above 75 MeV we used the recent data of Nagamiya *et al.*²⁷ for

0.8- and 2.1-GeV protons on C and NaF targets. They obtained differential cross sections at several angles from 10° to 30° and at energies from ~ 90 MeV up to a maximum energy corresponding to approximately the beam velocity. The cross sections in all cases fall off smoothly, with a considerable fraction of the cross section occurring at intermediate rapidities corresponding neither to projectile fragmentation nor to target fragmentation. We interpolated between the data for production of fragments by 2.1-GeV protons on carbon and by 2.1-GeV protons on NaF. We joined these curves on to the Maxwellians derived from the target fragmentation data in the previous paragraph.

In view of the uncertainties in the hadron flux and in the dependence of the cross sections on hadron energy, hadron type, and fragment energy, we believe the calculations show that there is no need to invoke exotic explanations for the events at $Z=1, 2,$ and 3 recorded in CR-39 detectors at 603 g/cm^2 . It is, in fact, rather surprising that the curves in Fig. 3 agree as well as they do with the measurements.

Consider next the differential energy spectra in Fig. 4. The solid curves were generated by dividing the range spectra in Fig. 3 by dE/dx . In this figure we compare our data and calculations with the deuteron spectrum (the dotted curve) calculated by Barber *et al.*¹² and with their measurements of deuterons and alphas and their upper limit on tritons. Their measurements were made at a depth of 747 g/cm^2 at Mt. Lemmon, Arizona, using a superconducting magnet, spark chambers, and scintillation counters to determine charge, rigidity, and time of flight. In order to compare their results with ours on the same graph, we have raised all their values by $e^{-603/125}/e^{-747/125} = 3.2$ to correct for the difference in hadron flux at the two locations. Our calculated deuteron spectrum fits both our low-energy data and the high-energy data of Barber *et al.* Their calculated deuteron spectrum falls off more rapidly than ours at energies below ~ 200 MeV because they took into account only quasifree and quasielastic production of deuterons, neglecting the large contribution at rapidities between that for target fragmentation and those for quasifree and quasielastic production.

The α flux reported by Barber *et al.* between 250 and 1500 MeV is based on observation of 8 particles after subtraction of an expected 4.8 spillovers from charge $Z=1$. Their data point is more than an order of magnitude higher than our calculated He spectrum, whereas our low-energy He data are reasonably consistent with our calculated He spectrum. Possibly they have underestimated the number of spillovers from charge $Z=1$.

V. DISCUSSION AND CONCLUSIONS

The major accomplishment of this study has been to show that CR-39 plastic track-recording sheets perform as well as we hoped they would, so that we can confidently invest in an array much larger in collecting area and in stack thickness, that can be maintained for a year or more at high altitude. The detection of $d+t$, He, and Li at rates roughly consistent with production in the atmosphere by secondary neutrons and protons is gratifying. It is worth pointing out that these are the first measurements made of energetic Li nuclei at mountain altitude and the first measurements of enough He nuclei to determine an energy spectrum at mountain altitude.

In this work we have measured event rates as low as $\sim 10 \text{ m}^{-2}\text{yr}^{-1}$ using CR-39. We can extend the technique down at least another two orders of magnitude, to rates $\sim 0.1 \text{ m}^{-2}\text{yr}^{-1}$, for events sufficiently highly ionizing to stand out above the background of $d, t,$ and He that we have reported. For comparison, the sea-level monopole search,¹⁰ using Lexan detectors, obtained an upper limit comparable to $0.1 \text{ m}^{-2}\text{yr}^{-1}$ but with a sensitivity so low that only particles with $Z/\beta \gtrsim 65$ could have been detected. Searches for quarks,² diquarks,²³ and massive baryons¹ have individually not been able to set limits lower than ~ 10 to $100 \text{ m}^{-1}\text{yr}^{-1}$. One powerful advantage of the CR-39 detector over electronic detectors is that it can accumulate events at an arbitrarily slow rate without being limited by spurious signals.

We presented evidence for the possible detection of several very highly ionizing particles. One event in Fig. 5, found in a stereomicroscopic scan of a 650-cm^2 area, penetrated the detector without significant change in ionization rate and had $Z/\beta \approx 25$. To be conservative, we assume that it could have been produced by a particle as light as beryllium, $Z=4$. The fluxes of products of secondary cosmic-ray interactions with air fall off too rapidly with charge and energy to account for this event. It is much more likely to have been produced during the 10-h flight from London to San Francisco. The orientations of the plastic sheets in the plane are not known. The apparent upward direction of the event (s_{top} slightly greater than s_{bottom}) would suggest that, if it did occur during the flight, the sheet in which this event was found was reversed from its orientation at White Mountain. The expected density of events with $Z \geq 4$ and $Z/\beta \geq 15$ accumulated in a 10-h plane flight at 250 g cm^{-2} is $\sim 13 \text{ m}^{-2}$ (column 5, Table I), which is quite consistent with our having found one such event in 650 cm^2 .

Our failure to find events with $30 \leq Z/\beta \leq 10^2$ in

an ammonia scan of the single-layer array led to an upper limit of $0.4 \text{ m}^{-2}\text{yr}^{-1}$ (95% C.L.) on the flux of such particles at the summit of White Mountain. From Eq. (1), we can make only the weak claim that the Centauro events could not have been caused by highly charged particles with $Z/\beta \sim 30$ to 100 and an interaction length greater than $\sim 10^3 \text{ g/cm}^2$. This upper limit on λ is for an assumed Centauro-event detection thickness of 50 g/cm^2 above the Chacaltaya emulsion chamber. If one takes 30 g/cm^2 instead of 50 g/cm^2 , then λ must be less than $\sim 600 \text{ g/cm}^2$.

This upper limit is more interesting when applied to superheavy magnetic monopoles such as are predicted by grand unified models.²⁹ With a mass on the order of the grand unification mass $\sim 10^{24} \text{ eV}/c^2$, such monopoles would be accelerated by galactic magnetic fields to energies $\sim 10^{20} \text{ eV}$ ($\beta \sim 10^{-2}$) and would penetrate the Earth's atmosphere with ease. Although cosmological and astrophysical arguments constrain the flux of such objects far more stringently than does our experiment, it is worth stating explicitly that our upper limiting flux applies to magnetic monopoles that have a mass such that they penetrate to mountain altitude and that have a velocity high enough that they ionize like an electrically charged particle with $Z/\beta \gtrsim 30$. From the calculations of Ahlen³⁰ and others,³¹ we infer that monopoles with $\beta \gtrsim 0.02$ would have been detected in our rapid scan. The monopole search of Fleischer *et al.*,¹⁰ with its threshold of $Z/\beta \gtrsim 65$, would not have detected such slow monopoles. Our limit of $0.4 \text{ m}^{-2}\text{yr}^{-1}$ is a factor $\sim 10^3$ lower than the previous limit¹ on slow, massive particles.

The two cylindrical holes detected in the 15-m^2 array by the ammonia scan are consistent with the high etching rates expected for particles with $Z/\beta \gtrsim 10^2$ but do not constitute evidence for such particles. They do provide a strong incentive for a multilayered, large-area, second-generation experiment, which we deployed at the summit station at White Mountain on 14 June 1981. (The multilayered stack will enable us to establish whether events such as the one in Fig. 5 with $Z/\beta \approx 25$ occurred at the summit or in the plane flight.) The goal of testing explanations of Centauro events in terms of highly ionizing particles now becomes within our reach.

ACKNOWLEDGMENTS

We are indebted to Don Buser and the staff of the University of California's White Mountain Research Station for their assistance in arranging for the exposure of the detectors in the summit cabin. We are also indebted to Ricardo Anda Peters, Director of the Instituto de Investigaciones Fisicas, Universidad Mayor de San Andres, La Paz, Bolivia, for his hospitality and assistance in arranging for a (continuing) exposure of our detectors in contact with the Brazil-Japan emulsion-chamber experiment. We thank Shoji Nagamiya for permission to quote his unpublished results (Ref. 27). This material is based upon work supported by the National Science Foundation under Grant No. PHY 78-24357 and the National Aeronautics and Space Administration under Grant No. NGR 05-003-376.

¹A. M. Bakich, L. S. Peak, P. A. Riley, and M. M. Winn, *Sixteenth International Cosmic Ray Conference, Kyoto, 1979, Conference Papers* (Institute of Cosmic Ray Research, University of Tokyo, Tokyo, 1979), Vol. VI, p. 53.

²L. W. Jones, *Rev. Mod. Phys.* **49**, 717 (1977).

³C. M. G. Lattes, Y. Fujimoto, and S. Hasegawa, *Phys. Rep.* **65**, 153 (1980).

⁴P. B. Price, F. Askary, and G. Tarlé, *Proc. Nat. Acad. Sci. U. S. A.* **77**, 44 (1980).

⁵R. W. Ellsworth, J. Goodman, G. B. Yodh, T. K. Gaiser, and T. Stanev, *Phys. Rev. D* **23**, 771 (1981).

⁶J. D. Bjorken and L. D. McLerran, *Phys. Rev. D* **20**, 2353 (1979).

⁷T. D. Lee and G. C. Wick, *Phys. Rev. D* **9**, 2291 (1974); A. B. Migdal, G. A. Sorokin, O. A. Markin, and I. N. Mishustin, *Phys. Lett.* **65B**, 423 (1977); A. R. Bodmer, *Phys. Rev. D* **4**, 1601 (1971).

⁸S. A. Chin and A. K. Kerman, *Phys. Rev. Lett.* **43**, 1292 (1979); A. K. Mann and H. Primakoff, *Phys. Rev. D*

22, 1115 (1980).

⁹P. C. M. Yock, *Ann. Phys. (N. Y.)* **61**, 315 (1970); *Int. J. Theor. Phys.* **2**, 247 (1969).

¹⁰R. L. Fleischer, H. R. Hart, G. E. Nichols, and P. B. Price, *Phys. Rev. D* **4**, 24 (1971).

¹¹B. G. Cartwright, E. K. Shirk, and P. B. Price, *Nucl. Instrum. Methods* **153**, 457 (1978).

¹²H. B. Barber, T. Bowen, D. A. De Lise, E. W. Jenkins, J. J. Jones, R. M. Kalbach, and A. E. Pifer, *Phys. Rev. D* **22**, 2667 (1980).

¹³R. L. Fleischer, P. B. Price, and R. M. Walker, *Nuclear Tracks in Solids* (University of California Press, Berkeley, 1975).

¹⁴G. Tarlé, S. P. Ahlen, and P. B. Price, *Nature* (London) (to be published).

¹⁵G. D. Westfall, R. G. Sextro, A. M. Poskanzer, A. M. Zebelman, G. W. Butler, and E. K. Hyde, *Phys. Rev. C* **17**, 1368 (1978).

¹⁶R. G. Korteling, C. R. Toren, and E. K. Hyde, *Phys. Rev. C* **7**, 1611 (1973).

- ¹⁷A. M. Poskanzer, G. W. Butler, and E. K. Hyde, *Phys. Rev. C* **3**, 882 (1971).
- ¹⁸L. M. Anderson, Jr., Lawrence Berkeley Laboratory Report No. LBL-6769, 1977 (unpublished).
- ¹⁹M. A. Shea, D. F. Smart, and J. R. McCall, *Can. J. Phys.* **46**, S-1098 (1968).
- ²⁰E. M. Friedlander, R. W. Gimpel, H. H. Heckman, Y. J. Karant, B. Judek, and E. Ganssauge, *Phys. Rev. Lett.* **45**, 1084 (1980).
- ²¹J. P. Alard, A. Baldit, R. Brun, J. P. Costilhes, J. Dhermain, J. Fargeix, J. Fraysse, J. Pellet, G. Roche, and J. C. Tamain, *Nuovo Cimento* **30A**, 320 (1975).
- ²²V. I. Bogatin, V. F. Litvin, O. V. Lozhkin, N. A. Perfilov, and Yu. P. Yakovlev, *Nucl. Phys.* **A260**, 446 (1976).
- ²³S. Hayakawa, *Cosmic Ray Physics* (Wiley, New York, 1969).
- ²⁴T. W. Armstrong, K. C. Chandler, and J. Barish, *J. Geophys. Res.* **78**, 2715 (1973).
- ²⁵D. Lal and B. Peters, in *Handbuch der Physik*, edited by S. Flugge (Springer, Berlin, 1967), Vol. 46, p. 551.
- ²⁶J. A. Gaidos, L. J. Gutay, A. S. Hirsch, R. Mitchell, T. V. Ragland, R. P. Scharenberg, F. Turkot, R. B. Willmann, and C. L. Wilson, *Phys. Rev. Lett.* **42**, 82 (1979).
- ²⁷S. Nagamiya, M. C. Lemaire, E. Moeller, S. Schnetzer, G. Shapiro, H. Steiner, and I. Tanihata, *Phys. Rev. C* **24**, 971 (1981).
- ²⁸W. T. Beauchamp, T. Bowen, A. J. Cox, and R. M. Kalbach, *Phys. Rev. D* **6**, 1211 (1972); G. L. Bashindzhagyan, L. I. Sarycheva, and N. B. Sinev, *Sixteenth International Cosmic Ray Conference, Kyoto, 1979, Conference Papers* (Ref. 1) Vol. VI, p. 143.
- ²⁹J. Preskill, *Phys. Rev. Lett.* **43**, 1365 (1979).
- ³⁰S. P. Ahlen, *Rev. Mod. Phys.* **52**, 121 (1980).
- ³¹J. D. Ullman, *Phys. Rev. Lett.* **47**, 289 (1981).